Carbohydrate Biosensors

DOI: 10.1002/anie.201300469

Mechanical Carbohydrate Sensors Based on Soft Hydrogel Particles**

Daniel Pussak, Daniela Ponader, Simone Mosca, Salomé Vargas Ruiz, Laura Hartmann, and Stephan Schmidt**

Label-free biosensors based on surface plasmon resonance (SPR), impedance spectroscopy, or quartz crystal microbalance (QCM) have become standard screening methods in the pharmaceutical industry.[1] The advantage of these techniques lies in their ability to probe biomolecular interactions with high selectivity without the risk of altering the binding affinity of the analyte molecules, for example by fluorescent labeling. The developments in this field are directed towards more affordable sensors with increased throughput and enhanced selectivity and sensitivity. Selectivity and sensitivity are still limited in particular for analyte molecules having dielectric constants close to water as the measured signal; for example, changes in the refractive index (SPR) become very small. Carbohydrates belong to this class of analytes and are exceptionally difficult to analyze because they also exhibit low affinity to their receptors.[2] On the other hand, understanding the biomolecular interactions of carbohydrates is increasingly important for various applications, such as drug development[3] or pathogen screening.[4] Direct force-based detection by atomic force microscopy (AFM), optical traps, or the like offer increased sensitivity and also precise information on the nature of the interaction; for example, discrimination between specific and unspecific binding.[5] Affinity biosensors could therefore take advantage of force-based detection; however, this approach has not been developed further owing to the low throughput of the involved techniques and their expensive instrumentation.

Our work describes a new force-based detection technique that can be easily adapted to construct various biosensors for high-throughput applications. As detection principle we used so-called soft colloidal probes (SCP) and the JKR model relating adhesion-induced mechanical deformation of SCPs to their surface energy.[6] The SCP surface energy serves as physical detection signal and is analogous to the resonance frequencies measured with SPR or QCM biosensors. To date the SCP technique has been used to measure surface energies arising from hydrophobic,[7] electrostatic,[8] and protein interactions[9] or to determine pressures on microscopic scale.[10] Herein, we describe a setup that advances this basic principle to now screen biomolecular interactions of various carbohydrate compounds. We provide detailed information on the synthesis of ligand/receptor functionalized SCPs based on polyethylenglycol (PEG) hydrogels and their optimal material parameters for sensitive carbohydrate detection. Finally, we discuss binding properties of multivalent carbohydrates determined by SCPs in comparison to SPR experiments. It is noteworthy that the SCP approach is quite general and not limited to carbohydrate analytes only.

In analogy to affinity-based biosensors, the SCP technique allows for direct binding assays as well as inhibition/competition assays. The general principle is as follows: Ligand- or receptor-functionalized SCPs are dispersed in buffer, and they sediment on the surface of a transparent glass slide that is functionalized with the respective binding partner. Upon contact, ligands and receptors bind, the SCPs adhere and form a distinct contact area with the glass surface (Figure 1 a,b). Highly deformable SCPs will exhibit large contact areas that can be conveniently detected by reflection interference contrast microscopy (RICM) to determine the surface energy W,

$$a^3 = 6\pi \frac{W}{E_{\text{eff}}} R^2 \tag{1}$$

where a is the radius of contact, R radius of the SCP, and $E_{\text{eff}} = [4E/3(1-\nu^2)]$ its effective elastic modulus, with ν the Poisson ratio and E the elastic modulus. The measurement of the SCP surface energy in the adhered state (Figure 1 b) corresponds to a direct binding assay where the analyte is positioned on the glass surface or the colloidal probe. Taking into account the surface densities of the binding partners, the specific ligand–receptor binding energy can be determined. The direct binding assays allow for the characterization of soft (bio)-interfaces but are not well suited for high-throughput screening applications, as each analyte would need to be conjugated to either of the two surfaces. Alternatively, SCP inhibition/competition assays (Figure 1 c,d) give fast and straightforward access to affinities of added analytes; that is, molecules that bind to either receptors or ligands. Upon addition of such additional analytes, they compete with the bonds that were formed upon adhesion of the SCP in the first step and thereby inhibit the interaction between the SCP and the surface. Depending on the concentration and the affinity of the analyte, the contact area and surface energy will decrease

[*] D. Pussak, D. Ponader, S. Mosca, S. V. Ruiz, Dr. L. Hartmann, Dr. S. Schmidt
MPI für Kolloid und Grenzflächenforschung
Am Mühlenberg 1, 14424 Potsdam (Germany)
E-mail: laura.hartmann@mpikg.mpg.de
stephan.schmidt@mpikg.mpg.de

[**] Financial support was granted by the German Research Foundation (DFG) through the Emmy Noether program (HA5950/1-1), and the collaborative research center (SFB) 765, the Center for Supramolecular Interactions (CSI) at Freie Universität Berlin and Max Planck Society. The authors thank P. H. Seeberger, P. Fratzl, M. Harrington, and T. Pompe for support and helpful discussions, and J. Erath is acknowledged for the RICM calibration procedure.

Supporting information for this article is available on the WWW under http://dx.doi.org/10.1002/anie.201300469.

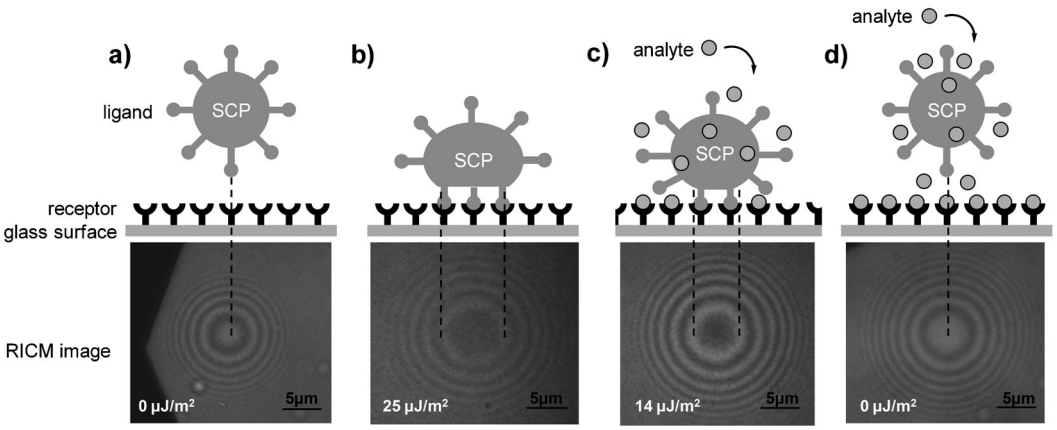

Figure 1. General principle: a) the ligand-functionalized probe comes into contact with the functionalized receptor surface, and b) upon contact with the receptor surface, ligand–receptor complexes form and induce mechanical deformation of the SCPs. c) Inhibition affinity assays by addition of analytes and detection of contact area until d) the probe detaches from the receptor surface. The RICM images show the contact area between the probe and the receptor surface, where the dark area in the center signifies the contact area. The upper sketch is not to scale, and the geometrical match between ligand and receptor surface is visually idealized.

(Figure 1 b–d). If all of the binding sites are occupied, the SCP detaches from the surface. Consequently, detection of contact area changes upon analyte addition yields the inhibitory concentration and thus the binding affinity of the analyte.

We have put the SCP measurement principle to the test by studying carbohydrate–protein interactions. As reference binding partners for the inhibition assays, we used the interaction between mannose (Man) as ligand and concanavalin A (ConA) as receptor. Chief requirements for robust and sensitive SCP biosensors are reduction of nonspecific surface interactions and the use of highly deformable SCP scaffolds. Recently, we introduced micrometer-sized SCPs composed of functional PEG hydrogels as probes for acid–base interactions that fulfill these criteria.[8] Here we chose long and flexible PEG macromonomers (8–20 kDa) resulting in highly compliant probes with an elastic modulus of 4–32 kPa (Supporting Information, Figure S1). The use of neutral and inert PEG scaffolds drastically reduces unspecific interactions but also complicates the bioconjugation with Man or ConA. To tackle this problem we adapted a surface chemistry route involving radical generation at the PEG backbone by UV irradiation.[11] This allowed the addition of carboxylic moieties into the PEG scaffold and subsequent functionalization with aminoethyl-linked Man or ConA by standard peptide coupling chemistry (Supporting Information, Figure S2).

We prepared two types of SCPs: a) Man-SCPs (4, 15, and 32 kPa) conjugated with Man-ligands; and b) ConA-SCPs (32 kPa) conjugated with ConA receptors (Figure 2 a,b). The homogeneity and degree of SCP bioconjugation was shown by confocal microscopy, ATR-FTIR, and amino acid analysis. The analysis showed that Man-SCPs present about one Man ligand for every 180 PEG repeat units, and that the ConA-SCPs were closely packed with ConA receptors (3.6×10^{16} ConA m^{-2}; Supporting Information, Figure S3). The second part of the SCP carbohydrate biosensor, which are are two types of glass surfaces, were prepared by silanization and coupling:[8] a) ConA-functionalized coverslips; and b) Man-functionalized coverslips (Supporting Information, Figure S4). The surface density of the ConA and Man-surfaces almost reached close packing (4×10^{15} ConA per m^2), as measured by amino acid analysis.

With this setup and using the 32 kPa SCPs we first performed direct binding assays and compared two experimental options: a) Man-SCP on ConA surface; and b) ConA-SCP on Man-surface (Figure 2). The surface energies of the SCPs were obtained measuring the SCP radii and contact area with the glass surface by RICM (Supporting Information, Figure S7). The data was then fitted with Equation (1), yielding the surface energy W of the SCPs (Figure 2 d). The surface energy obtained in direct binding of the Man-SCPs on ConA was 25 ± 2 μJ m^{-2} and 21 ± 2 μJ m^{-2} for the ConA-SCPs probes adhered to the Man surface. Both systems show similar surface energies indicating similar

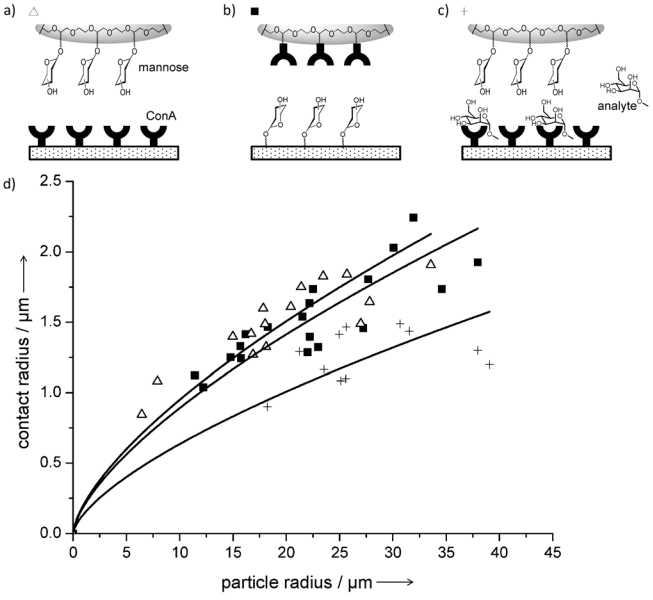

Figure 2. The different experimental configurations: a) SCPs with Man ligands and a ConA functionalized glass surface; b) SCPs with ConA and a Man-functionalized glass surface; c) addition of an inhibitor. d) Plot of the contact and particle radius and calculation of the surface energy W by fitting the data using Equation (1) (solid lines). ■ PEG-ConA, $W = 21.3 \pm 1.7$ μJ m^{-2}; △ PEG-Man, $W = 25.8 \pm 2.3$ μJ m^{-2}; + PEG-Man, $W = 7.3 \pm 1.4$ μJ m^{-2} (with 833 μM α-methyl-D-mannose).

densities of the binding partners as also shown by amino acid analysis as well as the independence of the binding partners location (either on SCP or glass slide). The experimental data can be put into context with the theoretical upper limit of the surface energy. The upper limit assumes the ideal situation in which all ConA binding pockets on the surface bind to a Man ligand with 5.2 kcal mol^{-1} contribution to the surface energy. With the ConA densities as measured by amino acid analysis, the upper surface energy limit would be 290 μJ m^{-2} and thus 10 times larger than the measured values. The stark difference between upper theoretical limit and measured value could be explained due to surface roughness on the order of 3 nm and non-ideal distribution of binding partners: The Man-ligands have a similar but random spacing compared to the ConA binding sites. Therefore the positions of most binding partners do not match entirely, overall reducing the probability of specific Man/ConA interactions (Supporting Information, Figure S5).

The specificity of the SCP binding was tested by addition of competitively binding sugar ligands into the measurement cell, for example, 10 mM α-Me-D-Man. At a critical level of competitive ligands, the SCP contact areas and surface energies completely vanish, thus indicating the specificity of the SCP-glass slide adhesion. Importantly, when adding α-Me-D-Man at lower concentrations up to 1 mM, the probes are still in contact with the glass surface (Figure 2d, cross markers) and surface energy gradually decreases with the concentration of added sugar (Figure 3). Therefore, depending on their concentration and affinity, the ConA receptors are inhibited only partially by the added sugar ligands. This can be directly visualized by the decreasing SCP contact areas upon sugar addition and quantified in terms of surface energy by the JKR approach.

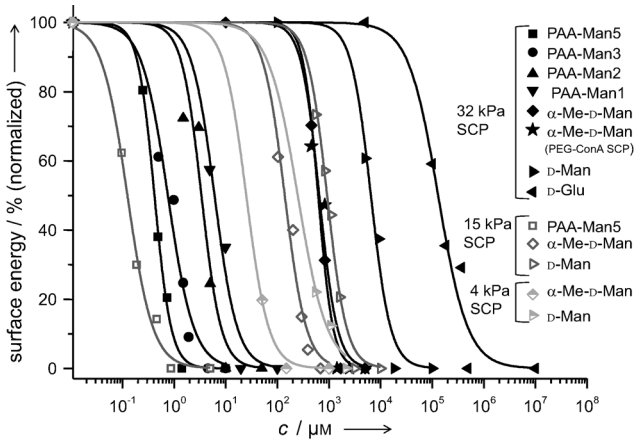

Figure 3. IC_{50} curves for various analytes inhibiting the Man/ConA interaction.

Owing to the specificity of the interaction and the concentration-dependent response of added sugar ligands, the SCP measurements can be used to perform competition/inhibition assays. This procedure involves variation of the analyte concentration and measurement of the respective SCP surface energies. Generally, these assays yield the half-maximal inhibitory concentration (IC_{50}) of the analyte as a measure of the analyte affinity. As analytes we used various monosaccharides: α-Me-D-Man, D-Man, and D-Glu with different binding affinities to ConA. All of the measurements were conducted with the SCP system shown in Figure 2a, using a Man-SCPs and ConA glass surfaces. Furthermore, we varied the SCP elastic modus (4, 15, and 32 kPa) to study the effect of PEG flexibility on the IC_{50}. With the direct binding between Man-SCP and ConA surface as a reference, the different analytes were added and for each concentration the decrease in surface energy was determined. Figure 3 shows the surface energies normalized direct binding experiment as a function of the inhibitor concentrations.

The normalized surface energy data showed a characteristic sigmoidal shape that was fitted with the Hill equation to obtain the IC_{50} values. To compare the IC_{50} obtained with the different SCPs we introduce a "relative affinity" that relates every analyte to the IC_{50} of α-Me-D-Man (Table 1). Clearly,

Table 1: IC_{50} values and relative activities normalized per Man-unit of sugar analyte as measured by SCP and SPR.

Inhibitor	SPR[13] IC_{50} [μM]	SCP-RICM[a] IC_{50} [μM]	Relative activity/Man
D-Glu	n.d.	$1.3\times10^{5}\pm1.9\times10^{4}$	0.005
D-Man	6500	6490 ± 500 (32 kPa SCP)	0.1
		920 ± 36 (15 kPa SCP)	0.15
		248 ± 81 (4 kPa SCP)	0.1
α-Me-D-Man	750	620 ± 20 (32 kPa SCP)	1
		140 ± 12 (15 kPa SCP)	1
		25 ± 2 (4 kPa SCP)	1
α-Me-D-Man[b]	750	650 ± 80	1
PAA-Man1	8	6.1 ± 0.7	101
PAA-Man2	5	3.4 ± 0.5	91
PAA-Man3	1	0.8 ± 0.1	258
PAA-Man5	n.d.	0.4 ± 0.1 (32 kPa SCP)	248
		0.12 ± 0.02 (15 kPa SCP)	234
		< 0.05 (4 kPa SCP)	> 100

[a] SCP measurements were conducted with 32 kPa probes if not denoted otherwise. [b] Inverted system PEG-ConA SCP versus Man-functionalized surface.

all of the carbohydrate inhibitors reduced the surface energy of the SCP owing to binding and inhibition of ConA. As expected, the monosaccharides show decreasing relative affinity from α-Me-D-Man, D-Man, to D-Glu, in agreement with calorimetric studies in solution.[12]

To show that the assay is also suitable for structurally and chemically different model drugs, we studied a set of multivalent glycooligomers based on monodisperse sequence-defined oligo(amidoamine) (PAA) scaffolds with a molecular weight of 2 kDa.[13] The PAAs carry up to five Man groups on a single chain of the same length (PAA-Man1, PAA-Man2, PAA-Man3, PAA-Man5). These structures show strong inhibition on ConA surfaces with IC_{50} values in the micromolar range and the same structural dependence as observed

in our previous SPR study.[13] It can be assumed that cooperative binding of these multivalent compounds could be noticed in the Hill plots, as observed in SPR and other studies.[13] However, all of the curves exhibit a slope on the order of two, regardless of mono- or multivalent Man-presentation. This could mean that the presence of an analyte not only inhibits a single receptor but also enhances the probability of unbinding adjacent receptors at the SCP surface. Thus, the observed cooperative inhibition is due to surface unbinding rather than binding cooperativity of the analytes themselves. Furthermore, the IC_{50} decreases by a factor of 25 when reducing the elastic modulus of the SCPs from 32 kPa to 4 kPa. This is likely to be due to an increased entropic gain upon unbinding the softer, more flexible PEG chains from the receptor surface.[14]

From a technical point of view, it is important to note that the relative affinities are similar regardless of the probes' elastic modulus and that they are in good agreement with the values obtained by SPR inhibition assays reported earlier (Table 1).[13] Thus, the method is robust and it delivered reproducible values also when comparing the inverted (Figure 2b) with non-inverted (Figure 2a) setup. Moreover, the glass surfaces can be easily regenerated by a few washing cycles with lectin binding buffer. Subsequent binding studies with α-Me-D-Man on the regenerated surfaces gave reproducible results (Supporting Information, Figure S6). The resolution in direct binding measurements for surface energy determination is limited by the inability of the method to differentiate between contact radius shifts smaller than 0.5 μm. However, the resolution limit can be significantly enhanced by using softer SCPs. As a proof of principle, we additionally prepared SCPs with 10 times smaller elastic moduli (0.3 kPa) by further reducing the photoinitiator concentration in the cross-linking step. The practical detection limit in surface energies for these SCPs is on the order of 0.1 $\mu J\,m^{-2}$, which most likely exceeds the sensitivity of the surface force apparatus and similar methods.

Overall, the SCP method is highly sensitive and shows reproducible results in carbohydrate screening assays, without the need of expensive instrumentation or consumables that apply to other label-free techniques, for example, metal-coated biochips or microcantilevers. Inhibition assays were conducted to study carbohydrate–lectin interactions using non-labeled analytes, yielding relative affinities that agreed well with those obtained from SPR measurements. Thus, the method has several useful characteristics especially for the characterization of analytes with low molecular mass and refractive indices close to water.

Furthermore, theoretical models suggest that the stiffness of a scaffold can affect the collective molecular interactions of attached binding partners.[15] It is also known that matrix elasticity has a pronounced effect on cell adhesion.[16] In principle, the binding of SCPs to a receptor surface represents a drastically reduced cell-matrix model system and indeed our measurement suggest that the elastic modulus can affect specific (un-)binding. Further SCP-based experiments with improved control over ligand/receptor spacing may help to understand the contribution of interface flexibility and multivalency in specific interactions.

Received: January 18, 2013
Revised: March 5, 2013
Published online: April 24, 2013

Keywords: bio-interfaces · biosensors · glycopolymers · microinterferometry · molecular recognition

[1] a) J. S. Daniels, N. Pourmand, *Electroanalysis* **2007**, *19*, 1239 – 1257; b) G. N. M. Ferreira, A.-C. da-Silva, B. Tomé, *Trends Biotechnol.* **2009**, *27*, 689 – 697.
[2] X. Q. Zeng, C. A. S. Andrade, M. D. L. Oliveira, X. L. Sun, *Anal. Bioanal. Chem.* **2012**, *402*, 3161 – 3176.
[3] a) C. R. Bertozzi, Kiessling, L. L. , *Science* **2001**, *291*, 2357 – 2364; b) H. Ghazarian, B. Idoni, S. B. Oppenheimer, *Acta Histochem.* **2011**, *113*, 236 – 247.
[4] M. D. Disney, P. H. Seeberger, *Chem. Biol.* **2004**, *11*, 1701 – 1707.
[5] D. J. Müller, Y. F. Dufrêne, *Nat. Nanotechnol.* **2008**, *3*, 261 – 269.
[6] K. L. Johnson, K. Kendall, A. D. Roberts, *Proc. R. Soc. London Ser. A* **1971**, *324*, 301 – 313.
[7] J. Erath, S. Schmidt, A. Fery, *Soft Matter* **2010**, *6*, 1432 – 1437.
[8] D. Pussak, M. Behra, S. Schmidt, L. Hartmann, *Soft Matter* **2012**, *8*, 1664 – 1672.
[9] V. T. Moy, Y. K. Jiao, T. Hillmann, H. Lehmann, T. Sano, *Biophys. J.* **1999**, *76*, 1632 – 1638.
[10] J. Bünsow, J. Erath, P. M. Biesheuvel, A. Fery, W. T. S. Huck, *Angew. Chem.* **2011**, *123*, 9803 – 9806; *Angew. Chem. Int. Ed.* **2011**, *50*, 9629 – 9632.
[11] W. J. Lee, D. K. Choi, Y. Lee, D. N. Kim, J. W. Park, W. G. Koh, *Sens. Actuators B* **2008**, *129*, 841 – 849.
[12] I. J. Goldstein, C. E. Hollerman, E. E. Smith, *Biochemistry* **1965**, *4*, 876 – 883.
[13] D. Ponader, F. Wojcik, F. Beceren-Braun, J. Dernedde, L. Hartmann, *Biomacromolecules* **2012**, *13*, 1845 – 1852.
[14] a) M. Mammen, S.-K. Choi, G. M. Whitesides, *Angew. Chem.* **1998**, *110*, 2908 – 2953; *Angew. Chem. Int. Ed.* **1998**, *37*, 2754 – 2794; b) C. Fasting, C. A. Schalley, M. Weber, O. Seitz, S. Hecht, B. Koksch, J. Dernedde, C. Graf, E.-W. Knapp, R. Haag, *Angew. Chem.* **2012**, *124*, 10622 – 10650; *Angew. Chem. Int. Ed.* **2012**, *51*, 10472 – 10498.
[15] a) T. R. Weikl, M. Asfaw, H. Krobath, B. Rozycki, R. Lipowsky, *Soft Matter* **2009**, *5*, 3213 – 3224; b) C. Forrey, J. F. Douglas, M. K. Gilson, *Soft Matter* **2012**, *8*, 6385 – 6392.
[16] A. J. Engler, S. Sen, H. L. Sweeney, D. E. Discher, *Cell* **2006**, *126*, 677 – 689.

